TU Wien
Department of Geodesy and Geoinformation
Research Area Höhere Geodäsie

Wrocław University of Environmental and Life Sciences

VMF3o: Enhanced Tropospheric Mapping Functions for Optical Frequencies

Janina Boisits[1], Daniel Landskron[1], Krzysztof Sosnica[2], Mateusz Drozdzewski[2], Johannes Böhm[1]

[1] TU Wien, Department of Geodesy and Geoinformation, Research Area Höhere Geodäsie, Vienna, Austria
[2] Wroclaw University of Environmental and Life Sciences, Institute of Geodesy and Geoinformatics, Wroclaw, Poland

21st International Workshop on Laser Ranging, 5 – 9 November 2018, Canberra, Australia

Outline

1. Developing VMF3o
2. Parameters of VMF3o
3. Testing and Validation
4. Test Results
5. Outlook

1. Developing VMF3o

- **VMF3o** = 'Vienna Mapping Functions 3 – **optical**'
- adapted from VMF3
  → well established MF for microwave techniques
- Coefficients a_h, b_h, c_h, and a_w, b_w, c_w
  estimated from **ray-tracing** analogously to VMF3
- Documentation
  → RADIATE: **Hofmeister, A. & Böhm, J. (2017)**
  → VMF3: **Landskron, D. & Böhm, J. (2018)**

$$MF_h(\varepsilon) = \frac{1 + \dfrac{a_h}{1 + \dfrac{b_h}{1 + c_h}}}{\sin\varepsilon + \dfrac{a_h}{\sin\varepsilon + \dfrac{b_h}{\sin\varepsilon + c_h}}}$$

$$MF_w(\varepsilon) = \frac{1 + \dfrac{a_w}{1 + \dfrac{b_w}{1 + c_w}}}{\sin\varepsilon + \dfrac{a_w}{\sin\varepsilon + \dfrac{b_w}{\sin\varepsilon + c_w}}}$$

RADIATE – new module for optical ray-tracing

- Refined piecewise-linear ray-tracing approach

Vertical interpolation levels		
Interval [km]	**Increment**	**Data source**
0 – 2	10 m	ECMWF
2 – 6	20 m	ECMWF
6 – 16	50 m	ECMWF
16 – 36	100 m	ECMWF
36 – 84	500 m	ECMWF / U.S. SA, 1976

$$N_h = N_{gaxs} \frac{T_d}{P_d} Z_d R_d \rho$$

$$N_w = N_{gws} \frac{\rho_w}{\rho_{ws}} - N_{gaxs} \frac{T_d}{P_d} \frac{Z_d}{Z} \frac{e}{T} \varepsilon$$

Mendes, V. & Pavlis, E. (2004)

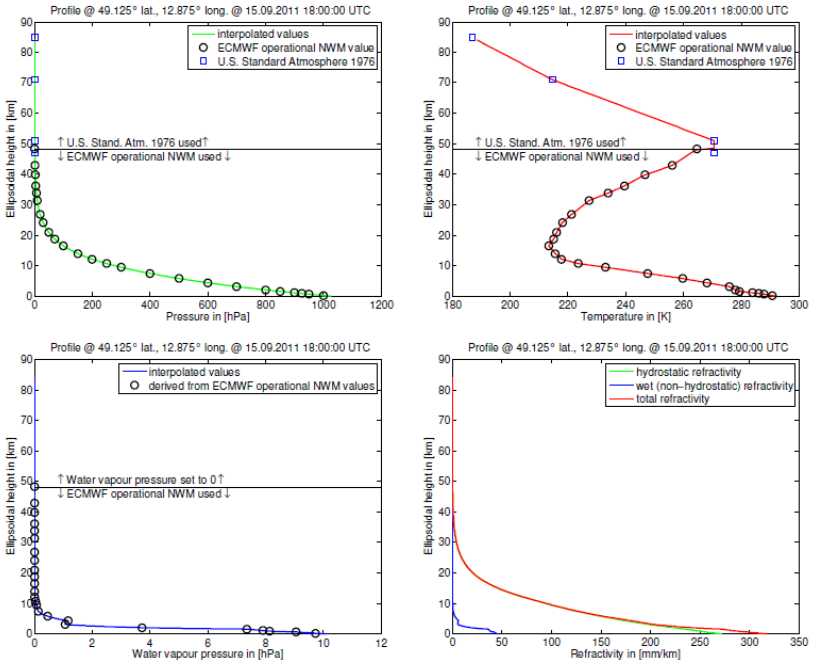

Hofmeister, A. (2016)

RADIATE – test of different wavelengths

- Differences of mapping factors using different wavelengths within azimuthal variation

  → wavelength **fixed to 532 nm**

	Wavelength 532 nm		Wavelength 1064 nm	
49.50° lat., 12.50° long., 01.01.2017 12:00:00 UTC				
ε [°]	MF_h	MF_w	MF_h	MF_w
5	$10.154_{\pm 0.012}$	$10.864_{\pm 0.089}$	$10.157_{\pm 0.012}$	$10.876_{\pm 0.089}$
7	$7.660_{\pm 0.007}$	$7.964_{\pm 0.041}$	$7.661_{\pm 0.007}$	$7.969_{\pm 0.041}$
10	$5.557_{\pm 0.004}$	$5.672_{\pm 0.019}$	$5.557_{\pm 0.004}$	$5.674_{\pm 0.019}$
15	$3.802_{\pm 0.002}$	$3.838_{\pm 0.008}$	$3.802_{\pm 0.002}$	$3.838_{\pm 0.008}$
49.50° lat., 12.50° long., 01.07.2017 12:00:00 UTC				
ε [°]	MF_h	MF_w	MF_h	MF_w
5	$10.131_{\pm 0.009}$	$10.845_{\pm 0.146}$	$10.134_{\pm 0.009}$	$10.856_{\pm 0.146}$
7	$7.649_{\pm 0.005}$	$7.957_{\pm 0.085}$	$7.650_{\pm 0.005}$	$7.962_{\pm 0.085}$
10	$5.552_{\pm 0.002}$	$5.670_{\pm 0.044}$	$5.553_{\pm 0.002}$	$5.672_{\pm 0.044}$
15	$3.801_{\pm 0.001}$	$3.837_{\pm 0.020}$	$3.801_{\pm 0.001}$	$3.838_{\pm 0.020}$

2. Parameters of VMF3o

- b_h, b_w, c_h, c_w estimated **once**
- a_h, a_w estimated **per epoch**

	a_h, a_w	b_h, b_w	c_h, c_w
Resolution of ray-traced delays			
Temporal	6h	Monthly	Monthly
Spatial	1°x1°	5°x5°	5°x5°
Elevation	5°	5°,7°,10°,15°	5°,7°,10°,15°
Availability of coefficients			
Resolution	1°x1° / 6h	SH *(lat,lon,doy)*	SH *(lat,lon,doy)*

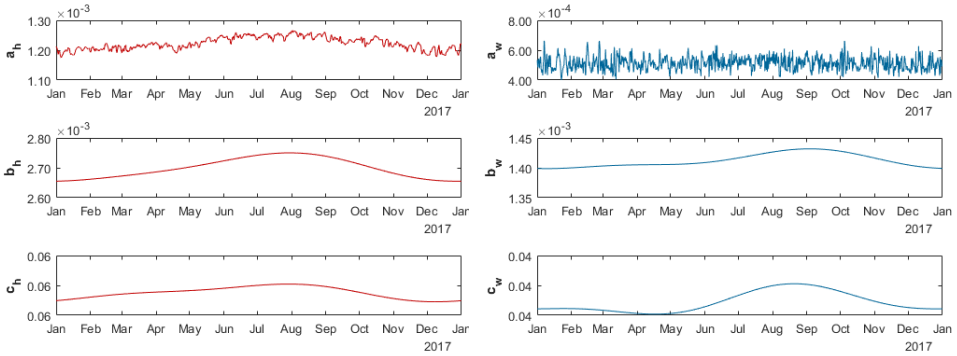

Time series of hydrostatic (**red**) and non-hydrostatic (**blue**) coefficients of VMF3o for the year 2017 at **49.50° lat., 12.50° long.**

a_h, a_w: 6h resolution in discrete grids
b_h, b_w, c_h, c_w: spherical harmonics expanded up to degree/order 12/12 with annual and semi-annual signals

3. Testing and Validation

- **Test data**
  - a_h, a_w: VMF3o files
  - b_h, b_w, c_h, c_w: SH coefficients
  - Period: 2005
  - Satellites: LAGEOS-1, LAGEOS-2
  - Resolution: 6h on 1°x1° grid
- **Software**
  - Bernese GNSS Software
    ver.5.3 dedicated for laser observation processing
- **Parameter sets**
  - 3 sets tested

	a_h, a_w	b_h, b_w, c_h, c_w	zhd	zwd
MP	MP	MP	MP	MP
VMF3o	VMF3o	VMF3o	MP	MP
VMF3ow	VMF3o	VMF3o	MP	VMF3o

4. Test Results

- Comparing slant delays at **station 7839** at **20° elevation angle**

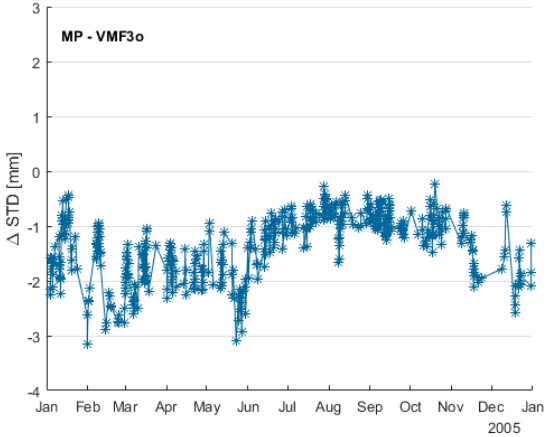

Difference of STD at 20° el. ang.
Solution **MP – VMF3o**
Station 7839

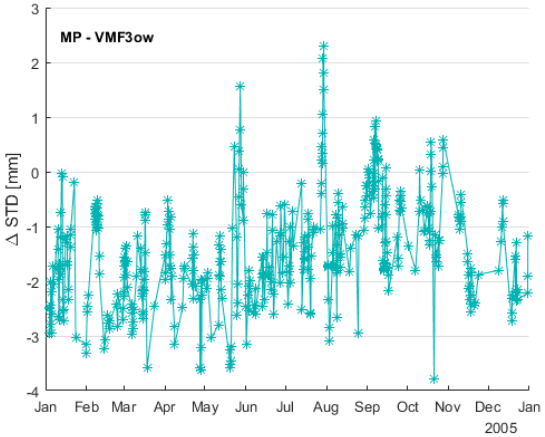

Difference of STD at 20° el. ang.
Solution **MP – VMF3ow**
Station 7839

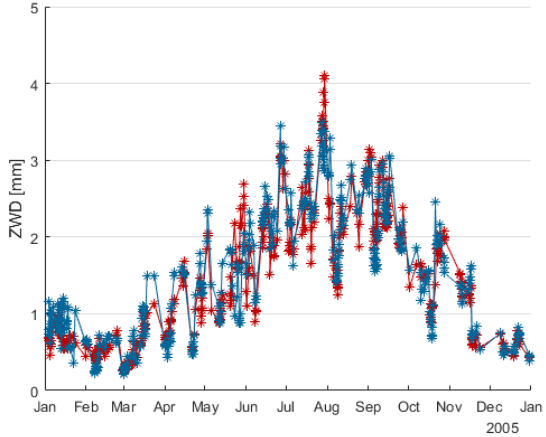

ZWD time series
MP (**red**) and **VMF3o** (**blue**)
Station 7839

Station Coordinates – MP vs. VMF3o

- Comparing station coordinate corrections from weekly solutions for **station 7839**

  → solution with smaller corrections compared to a priori coordinate plotted in foreground

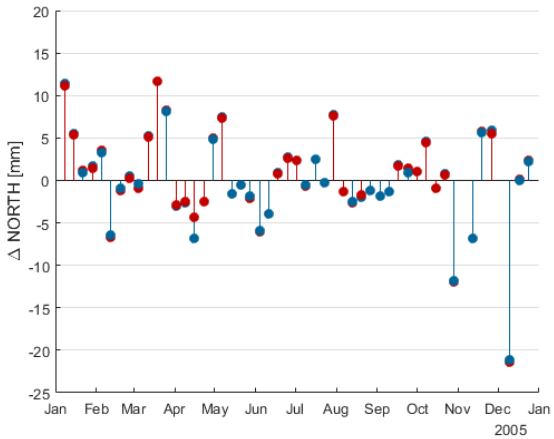

Correction of the **NORTH** component
MP (**red**) and **VMF3o** (**blue**)
Station 7839

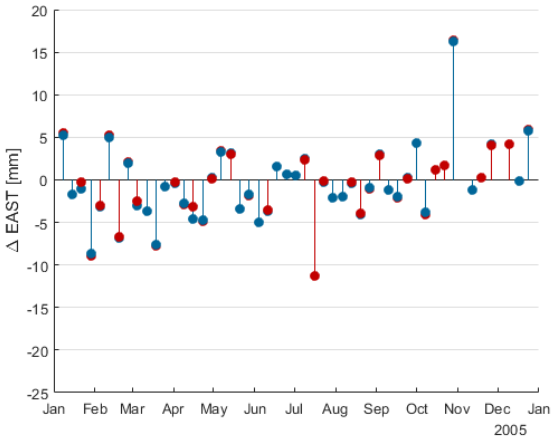

Correction of the **EAST** component
MP (**red**) and **VMF3o** (**blue**)
Station 7839

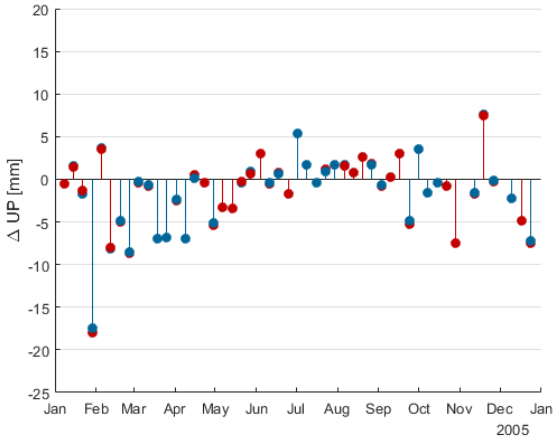

Correction of the **UP** component
MP (**red**) and **VMF3o** (**blue**)
Station 7839

Station Coordinates – MP vs. VMF3o

- Comparing station coordinate corrections from weekly solutions for **station 7839**

  → solution with smaller corrections compared to a priori coordinate plotted in foreground

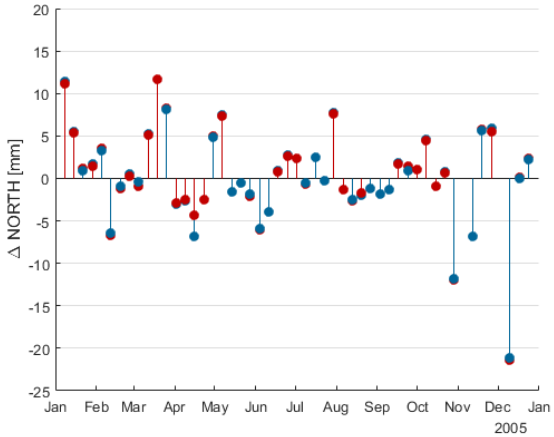

Correction of the **NORTH** component
MP (**red**) and **VMF3o** (**blue**)
Station 7839

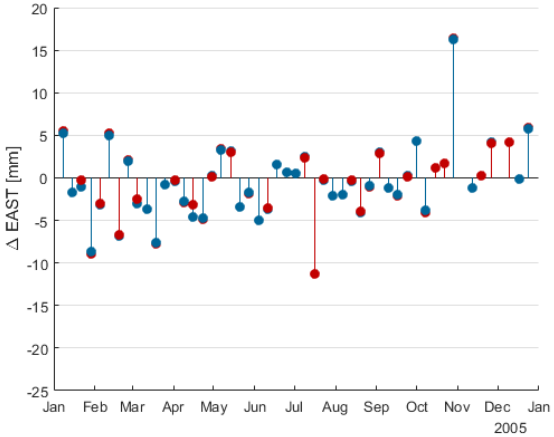

Correction of the **EAST** component
MP (**red**) and **VMF3o** (**blue**)
Station 7839

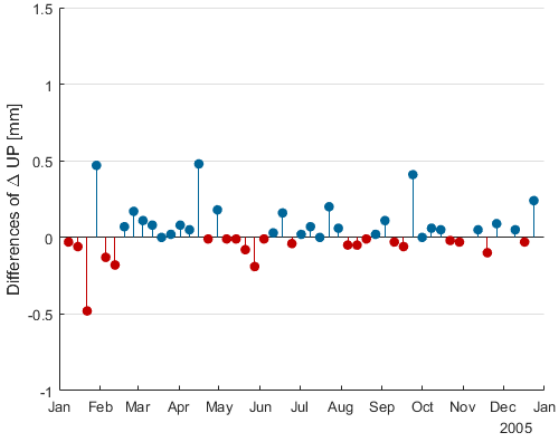

Differences of corrections of the **UP** component
MP – VMF3o
Station 7839

Station Coordinates – MP vs. VMF3ow

- Comparing station coordinate corrections from weekly solutions for **station 7839**

  → solution with smaller corrections compared to a priori coordinate plotted in foreground

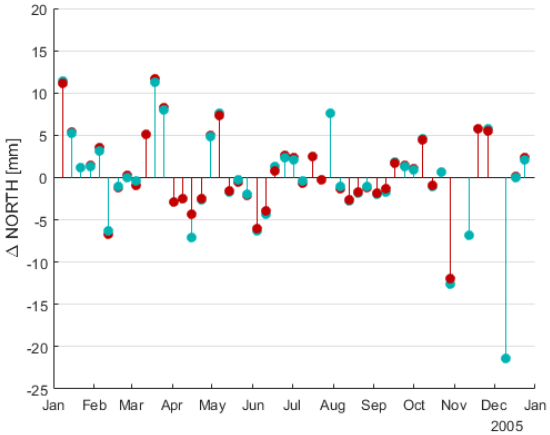

Correction of the **NORTH** component
MP (**red**) and **VMF3ow** (**turquois**)
Station 7839

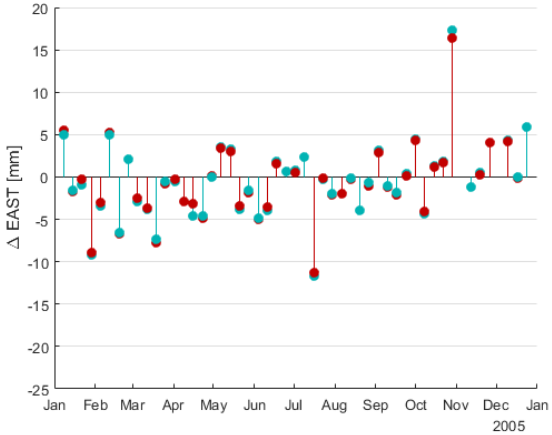

Correction of the **EAST** component
MP (**red**) and **VMF3ow** (**turquois**)
Station 7839

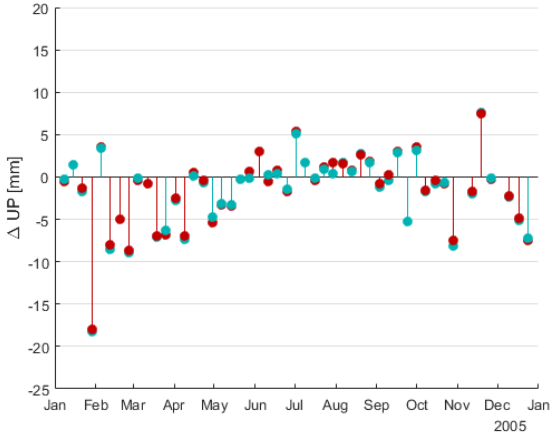

Correction of the **UP** component
MP (**red**) and **VMF3ow** (**turquois**)
Station 7839

Station Coordinates – MP vs. VMF3ow

- Comparing station coordinate corrections from weekly solutions for **station 7839**

  → solution with smaller corrections compared to a priori coordinate plotted in foreground

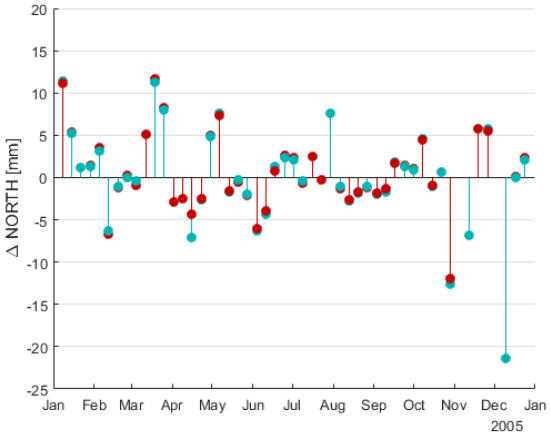

Correction of the **NORTH** component
MP (**red**) and **VMF3ow** (**turquois**)
Station 7839

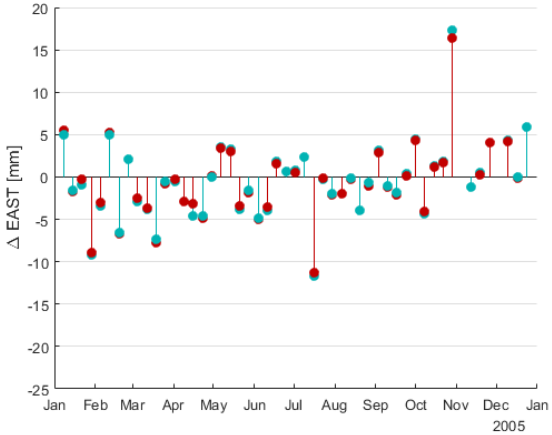

Correction of the **EAST** component
MP (**red**) and **VMF3ow** (**turquois**)
Station 7839

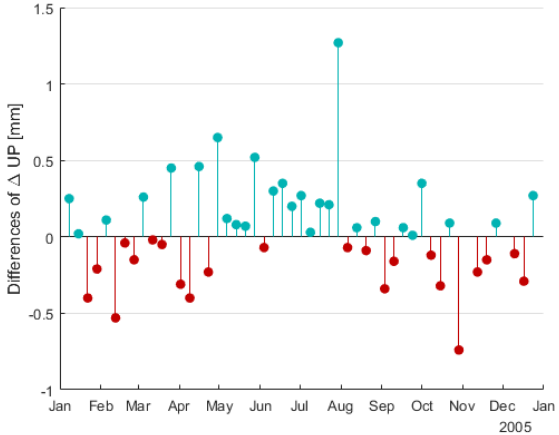

Differences of corrections of the **UP** component
MP – VMF3ow
Station 7839

Residual Analysis

- Comparing mean values of **absolute observation residuals** per station

	MP – VMF3o	MP – VMF3ow		MP – VMF3o	MP – VMF3ow
1864	-0.009	-0.001	**7810**	-0.049	-0.105
1873	0.005	0.011	**7811**	0.002	0.007
1884	0.005	0.048	**7824**	0.011	-0.123
7080	-0.037	-0.006	**7825**	-0.046	-0.074
7090	-0.028	-0.065	**7832**	-0.044	0.021
7105	-0.013	0.001	**7838**	0.020	0.075
7110	0.012	0.005	**7839**	-0.005	0.007
7237	0.003	0.013	**7840**	-0.007	0.015
7249	0.006	0.071	**7841**	0.007	0.000
7405	-0.003	-0.012	**7941**	0.008	0.051
7501	-0.051	-0.015	**8834**	0.014	0.022

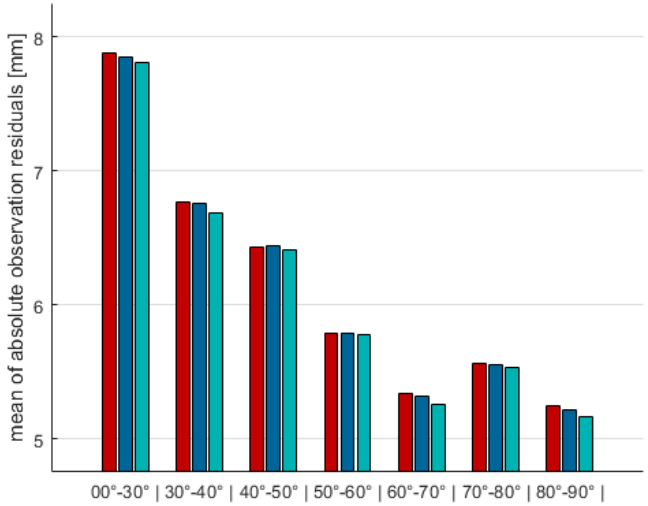

Mean value of **absolute observation residuals** classified into 7 bins of **elevation angles**
MP (**red**), **VMF3o** (**blue**) and **VMF3ow** (**turquois**)
Station 7941

5. Outlook

- Ray-tracing **directly at SLR stations**
  → mitigating error sources
  → save computation time and disk space
- Further investigations of **VMF3ow** solution
- Investigations of the effect of applying **horizontal gradients**
- VMF3o files for 2017 at vmf.geo.tuwien.ac.at/trop_products/SLR_prelim/

  → feel free to test data set!

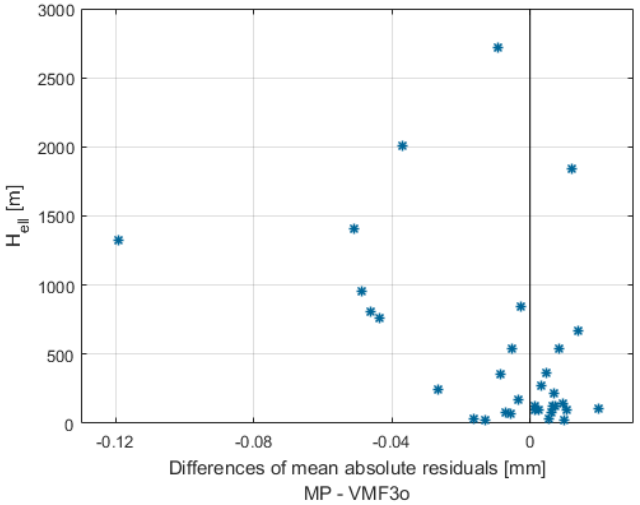

Differences of **mean values of absolute observation residuals** plotted against **station height**

→ grid interpolation and height extrapolation as major error sources

References

- **Hofmeister, A. (2016).** Determination of path delays in the atmosphere for geodetic VLBI by means of ray-tracing. *Ph.D. thesis, Department of Geodesy and Geoinformation, Faculty of Mathematics and Geoinformation, TU Wien*. http://resolver.obvsg.at/urn:nbn:at:at-ubtuw:1-3444
- **Hofmeister, A. & Böhm, J. (2017).** Application of ray-traced tropospheric slant delays to geodetic VLBI analysis. *J Geod (2017) 91: 945.* https://doi.org/10.1007/s00190-017-1000-7
- **Landskron, D. & Böhm, J. (2018).** VMF3/GPT3: refined discrete and empirical troposphere mapping functions. *J Geod (2018) 92: 349.* https://doi.org/10.1007/s00190-017-1066-2
- **Mendes, V. & Pavlis, E. (2004).** High-accuracy zenith delay prediction at optical wavelengths. *Geophys. Res. Lett. 31, L14602*. https://doi.org/10.1029/2004GL020308
- **Mendes, V., Prates, G., Pavlis, E., Pavlis D. & Langley, R. (2002).** Improved mapping functions for atmospheric refraction correction in SLR. *Geophys. Res. Lett. 29(10)*. https://doi.org/10.1029/2001GL014394